

See discussions, stats, and author profiles for this publication at: <https://www.researchgate.net/publication/349230660>

# Hands-on Experiment for Modeling the Baumgartner Jump Using Free-Fall Kinematics with Drag

Article in *The Physics Teacher* · February 2021

DOI: 10.1119/10.0003464

CITATION

1

READS

468

3 authors:



Alexander Gössling

Marienschule Bielefeld

26 PUBLICATIONS 364 CITATIONS

SEE PROFILE



Sebastian Becker-Genschow

University of Cologne

70 PUBLICATIONS 493 CITATIONS

SEE PROFILE



Jochen Kuhn

Ludwig-Maximilians-University of Munich

416 PUBLICATIONS 5,885 CITATIONS

SEE PROFILE

# Hands-on Experiment for Modeling the Baumgartner Jump Using Free-Fall Kinematics with Drag

Cite as: Phys. Teach. **59**, 111 (2021); <https://doi.org/10.1119/10.0003464>

Published Online: 11 February 2021

Alexander Gössling, Sebastian Becker, and Jochen Kuhn



View Online



Export Citation

# Hands-on Experiment for Modeling the Baumgartner Jump Using Free-Fall Kinematics with Drag

Alexander Gössling, Technische Universität Kaiserslautern, and Institut für Schule, Erziehungs- und Fachwissenschaften, Bielefeld, Germany  
Sebastian Becker and Jochen Kuhn, Technische Universität Kaiserslautern, Physics Education Research Group, Kaiserslautern, Germany

Supersonic free-fall jumps are excellent examples of kinematics in the context of drag. They have attracted a lot of media, public, and scientific interest.<sup>1–4</sup> In 2012, Felix Baumgartner jumped from a height of approximately 38.969 km. During his flight he reached a top speed of 373 m/s, becoming the first human to travel faster than the speed of sound outside of an airplane.<sup>5</sup> Since everyday topics are known to motivate students (e.g., Kuhn and Müller<sup>6</sup>), the topic of Baumgartner's jump seems to be very well suited for teaching kinematics in the context of drag.

Our motivation is to recreate the real jump of Baumgartner in a laboratory experiment, combining this interesting topic with hands-on experience using mobile video analysis. The experiment can be performed by students themselves using everyday materials. The data can be acquired and analyzed with video analysis software on a tablet computer. The limitations of this hands-on experiment will be discussed on the basis of quantitative modeling in this paper.

## Hands-on experiment using video analysis on tablet computers

The setup of the hands-on experiment is shown in Fig. 1. It consists of a glass cylinder (diameter 4.4 cm) filled with glycerol (6 cm height) and rape oil (18.5 cm height). The fluids do not mix and form separate layers due to their different densities. A small steel sphere (diameter 0.795 cm) can fall through both fluids. These two fluids correspond to the troposphere and the stratosphere in Baumgartner's jump; the steel sphere represents Baumgartner (see left panel of Fig. 1). A similar setup has also been suggested for the context of skydiving.<sup>7</sup>

Data acquisition was carried out by video analysis as described in the literature.<sup>8</sup> First, a video of the fall was recorded with the internal camera of a tablet computer (Apple iPad) using a frame rate of 120 fps. Second, the position of the sphere in the video was automatically tracked by the free user-friendly video analysis app Viana for iOS.<sup>9</sup> The height  $y$  and the  $y$ -component of the velocity as a function of time can

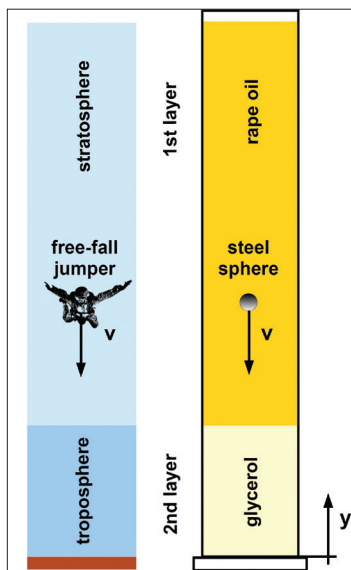


Fig. 1. Sketch of a free-fall jumper (left) and a steel sphere (right) falling through two different media. Note: The zero points of height  $y$  represent the surface of Earth and the bottom of the glass cylinder, respectively.

either be directly displayed by the app (not shown here) or the data can be easily exported. The data are shown in Fig. 2. For clarity, only every third data point is displayed.

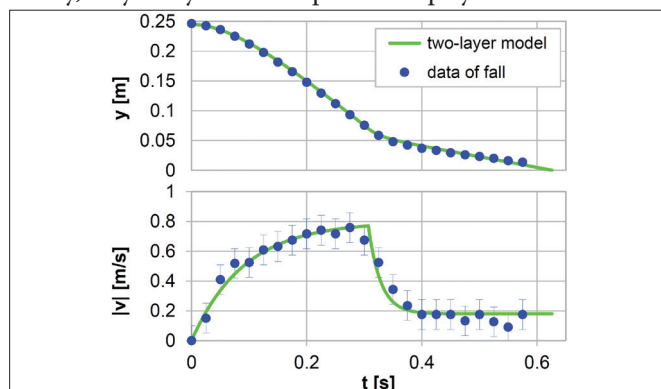


Fig. 2. The “data of fall” (obtained by video analysis) and the “two-layer modeling” of a falling steel sphere. Height (top panel) and speed (bottom panel) as a function of time. The measurement errors of  $\Delta y = 0.001$  m and  $\Delta v = 0.1$  ms<sup>-1</sup> were estimated from five repetitions of the experiment.

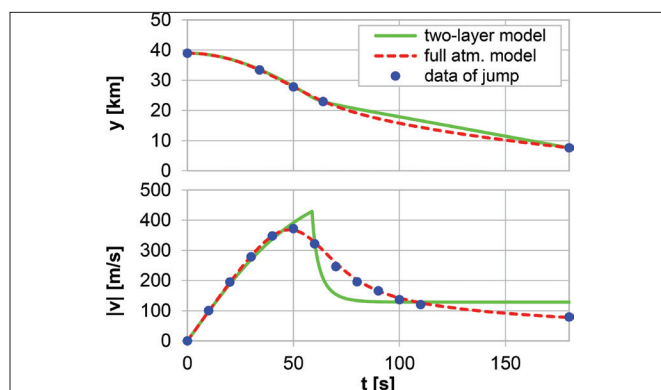


Fig. 3. The “data of jump” (reproduced from Stratos RB data<sup>5</sup>), the “two-layer modeling,” and the “full atmospheric modeling” of Baumgartner's jump. Height (top panel) and speed (bottom panel) as a function of time.

The height decreases with increasing time, while the speed increases. The steel sphere falls faster in rape oil than in glycerol due to the different viscosities of the fluids. Kinks at  $t = 0.30$  s in both curves indicate that the sphere passes from one medium to the other. Due to friction, the sphere does not become faster after a certain time in each medium but continues to drop uniformly at a constant speed. In the figure, terminal velocities for each medium could be observed at  $\sim 0.8$  m/s and  $\sim 0.2$  m/s, respectively. After  $t = 0.63$  s at  $y = 0$  m, the sphere reaches the bottom of the glass cylinder.

The behavior of the falling steel sphere can be explained by taking the media and the acting forces into account. Within each medium (rape oil or glycerol) the gravity force points down towards Earth, and the (small) buoyancy force and the drag force point upwards. The gravity force and the buoyancy

**Table I. Parameters for modeling a falling steel sphere and Baumgartner's jump within a two-layer model. Some parameters were kept fixed in the model because they are well known from literature, while others are left to fit to the data.**

exp	mass $m$	time $t_{12}$	medium (1)	$\frac{m_{\text{fluid}}^{(1)} - m}{m} \cdot g$	$\frac{k^{(1)}}{m}$ or $\frac{\tilde{k}^{(1)}}{m}$	medium (2)	$\frac{m_{\text{fluid}}^{(2)} - m}{m} \cdot g$	$\frac{k^{(2)}}{m}$ or $\frac{\tilde{k}^{(2)}}{m}$
falling sphere	0.00207 kg (fixed)	0.31 s (fitted)	rape oil	-8.67 m/s <sup>2</sup> (fixed)	10.9 1/s (fitted)	glycerol	-8.24 m/s <sup>2</sup> (fixed)	45.6 1/s (fitted)
Baumgartner	118 kg (fixed)	59 s (fitted)	strato-sphere	-9.81 m/s <sup>2</sup> (fixed)	$0.33 \times 10^{-4}$ 1/m (fitted)	tropo-sphere	-9.81 m/s <sup>2</sup> (fixed)	$5.93 \times 10^{-4}$ 1/m (fitted)

force remain constant, but the drag force is proportional to the velocity. After some time, the total force equals zero and the fall continues with the first terminal velocity, as observed in the data. The drag force increases abruptly when entering the second medium, and thus the sum of the drag force and the buoyancy force is greater than the gravity force. As a consequence, the speed suddenly decreases until force equilibrium is reached. The fall is again continued with the second terminal velocity.

## Two-layer modeling

We used a two-layer model, that is, a system consisting of two different media with different, uniform densities (see Fig. 1) in order to fit the measured data. This model might also be of interest for advanced students. For each layer, denoted as 1 or 2, one can specify the acting forces<sup>10</sup>:

$$F^{(1,2)} = F_g + F_b^{(1,2)} + F_d^{(1,2)} =$$

$$m \cdot \ddot{y}^{(1,2)} = -m \cdot g + m_{\text{fluid}}^{(1,2)} \cdot g + F_d^{(1,2)}. \quad (1)$$

Here,  $F_g$  represents the gravity force,  $F_b^{(1,2)}$  the buoyancy force,  $F_d^{(1,2)}$  the drag force,  $m$  the mass of the falling object, and  $m_{\text{fluid}}^{(1,2)}$  the mass of the displaced fluid.

The magnitude of the drag force varies with the speed  $v$  in a complicated way. For a first approximation, one can write the drag force as a linear or a quadratic term in  $v$ . The dimensionless Reynolds number<sup>11-13</sup>

$$R = \frac{\rho \cdot v \cdot d}{\eta} \quad (2)$$

provides a hint about which kind of drag force has to be used. For small Reynolds numbers the linear term has to be considered, and for large Reynolds numbers the quadratic term has to be taken into account. In Eq. (2),  $d$  denotes the diameter,  $v$  the speed of the moving object,  $\rho$  the density, and  $\eta$  the dynamic viscosity of the medium.

In the case of the falling sphere,  $R$  is assumed to be small,<sup>12</sup> so the drag force for viscous media is given by Stokes' law,<sup>11-14</sup>

$$F_d^{(1,2)} = k^{(1,2)} \cdot \dot{y}. \quad (3)$$

The time when the sphere changes from one medium to the other is denoted by  $t_{12}$ . Equation (1) was solved numerically using Euler's method for each layer.<sup>15</sup> In order to model the observed data, the parameters  $k^{(1,2)}$  and  $t_{12}$  were fit to the data.<sup>16</sup> All modeling parameters are summarized in Table I. The resulting time-height data and time-speed data for the

falling sphere are shown in Fig. 2 together with the measured data. The agreement between the theory and the experiment is quite good. The goodness of fit (relative root mean squared error [RRMSE]) for both datasets yields RRMSE = 0.149.

## Baumgartner's jump and further modeling

The real data for Baumgartner's jump<sup>5</sup> are shown in Fig. 3. The top panel represents the altitude of Baumgartner, while the bottom panel shows his speed of flight (in  $y$ -direction). In the first phase of his fall, Baumgartner's speed increases almost linearly, with an acceleration of  $g$ . After  $t \approx 30$  s his acceleration starts to decrease, and his speed reaches a maximum of  $v = 373$  m/s at  $t \approx 50$  s. In the second phase of his fall his speed decreases rapidly and converges to a terminal velocity of  $v = 80$  m/s at  $t = 180$  s. At that time Baumgartner was at an altitude of  $y = 7.619$  km.

The data for Baumgartner's real jump show striking similarity to the data and modeling of the hands-on experiments in Fig. 2. Again, the maximum speed of Baumgartner's jump at  $t = 50$  s can be explained by the density change in two media, in this case between the stratosphere and the troposphere. In contrast to the hands-on experiment, the density changes continuously from the stratosphere to the troposphere (exponential decay, see also below). As a consequence, the maximum in the time-speed diagram in Fig. 3 is rounded.

The next step is to test the applicability of the two-layer model on a quantitative level. We again use two-layer modeling (see section above), where the first layer is the stratosphere and the second layer is the troposphere. In this model, both layers have a constant density. Instead of Stokes' law, high-speed drag has to be considered for Baumgartner's jump because the Reynolds number is very large.<sup>17</sup> The high-speed drag is described by the formula<sup>11,12</sup>

$$F_d^{(1,2)} = \tilde{k}^{(1,2)} \cdot \dot{y}^2. \quad (4)$$

All modeling parameters are shown in Table I. The parameters for  $\tilde{k}^{(1,2)}$  were adjusted in order to fit the data.<sup>18</sup> While the time-height data can be modeled quite accurately, the time-speed data can only be reproduced for the first phase of Baumgartner's jump. It is not possible to obtain a rounded maximum within the two-layer model (goodness of fit for both datasets: RRMSE = 0.207).

The agreement with the data, that is, a rounded maximum, can be greatly improved (RRMSE = 0.024) by using an exponentially decaying density with increasing altitude instead of two layers with two constant values for the density (see Fig. 3, full atm. model). Details on the modeling can be found in Ref. 19.

## Conclusions

We presented a hands-on experiment to model Baumgartner's free-fall jump. The experiment consists of a steel sphere (Baumgartner), a layer of rape oil (stratosphere), and a layer of glycerol (troposphere). Data acquisition and analysis were carried out with the use of a free video analysis app (Viana) on a tablet computer. The hands-on experiment can adapt key points of the real jump, that is, the time-speed and the time-height values, on a qualitative level and is therefore very well suited for university or school use. Furthermore, we were able to show by theoretical modeling that the two-layer approach of the hands-on experiment also yields adequate quantitative agreement with the real jump data. However, a more convincing agreement could be achieved by using a full atmospheric model (exponential varying density) instead of two layers with fixed densities. The use of a smartphone as an experimental tool can be helpful during learning. As research shows, learning with mobile video analysis could increase conceptual understanding<sup>20,21</sup> while decreasing irrelevant cognitive effort and negative emotions.<sup>20,22</sup>

## Acknowledgment

The authors gratefully acknowledge P. Klein for very helpful discussions.

## References

1. J. M. Colino, J. Barbero, and F. J. Tapiador, "Dynamics of a skydiver's epic free fall," *Phys. Today* **67**, 64 (April 2014); J. M. Colino and A. J. Barbero, "Quantitative model of record stratospheric free fall," *Eur. J. Phys.* **34**, 841 (April 2013).
2. A. Müller, "Supersonic jump," *Phys. Teach.* **51**, 14 (Jan. 2013).
3. T. Corvo, "An analytical solution to the extreme skydiver problem," *Phys. Teach.* **57**, 289 (May 2019).
4. M. Guerster and U. Walter, "Aerodynamics of a highly irregular body at transonic speeds – Analysis of STRATOS flight data," *PLOS ONE* **12**(12), e0187798 (Dec. 2017).
5. Stratos RB, *Summary Report: Findings of the Red Bull Stratos Scientific Summit* (California Science Center, Los Angeles, 2013). Available at: [https://issuu.com/redbullstratos/docs/red\\_bull\\_stratos\\_summit\\_report\\_final\\_050213](https://issuu.com/redbullstratos/docs/red_bull_stratos_summit_report_final_050213), accessed May 7, 2019.
6. J. Kuhn and A. Müller, "Context-based science education by newspaper story problems: A study on motivation and learning effects," *Perspect. Sci.* **2**, 5 (Jun. 2014).
7. J. C. Leme, C. Moura, and C. Costa, "Steel spheres and skydiver – Terminal velocity," *Phys. Teach.* **47**, 531 (Nov. 2009).
8. S. Becker, P. Klein, and J. Kuhn, "Video analysis on tablet computers to investigate effects of air resistance," *Phys. Teach.* **54**, 441 (Oct. 2016).
9. Viana for iOS, Freie Universität Berlin. Available at <https://goo.gl/4RWv8g>, accessed May 7, 2019.
10. W. Demtröder, *Mechanics and Thermodynamics*, 1st ed. (Springer, Berlin, 2017), p. 220ff.
11. L. D. Landau and E. M. Lifshitz, *Fluid Mechanics*, 2nd ed. (Pergamon Press, Oxford, 1987), p. 61ff.
12. J. R. Taylor, *Classical Mechanics* (University Science Books, 2005), p. 43ff.
13. M. T. Mawhinney, M. K. O'Donnell, J. Fingerut, and P. Habdas, "Measuring drag force in Newtonian liquids," *Phys. Teach.* **50**, 173 (March 2012).
14. Viscous drag (Stokes):  $k^{(1,2)} = 6\pi\eta^{(1,2)}r$ , where  $\eta^{(1)}$  denotes the

dynamic viscosity of rape oil,  $\eta^{(2)}$  the dynamic viscosity of glycerol, and  $r$  the radius of the sphere. This formula is only strictly valid for small Reynolds numbers  $R \lesssim 1$ .<sup>11-13</sup>

15. R. Müller, *Klassische Mechanik – vom Weitsprung zum Marsflug*, 2nd ed. (De Gruyter, Berlin, 2010), p. 149ff [in German]; the  $y$ -component of the velocity  $v$  and the height  $y$  for each layer can be calculated using the following recursive expressions:

$$v(t + \Delta t) = \dot{y}(t + \Delta t) = \dot{y}(t) + \frac{F}{m} \cdot \Delta t,$$

$$y(t + \Delta t) = y(t) + v(t) \cdot \Delta t.$$

16. Model of falling sphere: For this experiment the Reynolds numbers<sup>12</sup> for the falling sphere in rape oil and glycerol yield  $R^{\text{rape oil}} \sim 50$  and  $R^{\text{glycerol}} \sim 1$ , respectively. Since Stokes' law is only applicable for small Reynolds numbers, it is only possible to determine the dynamic viscosity of glycerol in reasonable agreement with literature data  $\eta_{\text{lit}}^{(2)} = 1.48$  Pas from the fitted parameter  $k^{(2)}$ . For rape oil, extensions to Stokes' law have to be used (not done here), which are valid for larger Reynolds numbers, in order to extract values for the dynamic viscosity of rape oil.<sup>11,12</sup>
17. High-speed drag:  $\tilde{k}^{(1,2)} = 1/2 C_D \rho^{(1,2)} A$ , where  $\rho^{(1)}$  denotes the density of the stratosphere,  $\rho^{(2)}$  the density of the troposphere,  $A$  the projected surface area of Baumgartner, and  $C_D$  the drag coefficient.  $A$  and  $C_D$  are assumed to be constant during the fall; that is, Baumgartner's flight position does not change (which is not the case in reality).<sup>1</sup> The formula for high-speed drag is valid for large Reynolds numbers  $R \lesssim 2300$ .<sup>11,12</sup> For Baumgartner's jump, the formula above is applicable because  $R^{\text{Baumgartner}} \sim 600000 \gg 2300$ .
18. Model of Baumgartner's jump (two-layer model): From the fitted  $k$ -values, one can derive the densities of the stratosphere  $\rho^{\text{stratosphere}}^{(1)} = 0.010 \text{ kg/m}^3$  and the troposphere  $\rho^{\text{troposphere}}^{(2)} = 0.187 \text{ kg/m}^3$ . These values are in reasonable agreement (deviation  $\sim 0.25$ ) with medium densities of the U.S. standard atmosphere.
19. Model of Baumgartner's jump (full atmospheric model) analogue compared to a description of the model of Kittinger's jump<sup>15</sup>:  $m = 118 \text{ kg}$  (fixed);  $(m_{\text{fluid}}^{(1,2)} - m/m)g = -9.81 \text{ m/s}^2$  (fixed);  $\rho(y) = \rho_0 \cdot e^{-(ay+by^2)}$  with  $\rho_0 = 1.225 \text{ kg/m}^3$ ,  $a = 0.098 \text{ km}^{-1}$ , and  $b = 0.0015 \text{ km}^{-2}$  (fitted to U.S. standard atmosphere in 1976 from 0 km to 40 km);  $\tilde{k}/m = 1/(2m) C_D A \rho(y) = 1/(2m) C_D A \rho_0 e^{-(ay+by^2)} = \kappa e^{-(ay+by^2)}$  with  $\kappa = 0.0039 \text{ m}^{-1}$  (fitted). The value of  $\kappa$  corresponds to a value of  $C_D A = 0.75 \text{ m}^2$  and is in good agreement with values reported for Baumgartner's jump.<sup>1</sup>
20. S. Becker, A. Gößling, P. Klein, and J. Kuhn, "Using mobile devices to enhance inquiry-based learning processes," *Learn. Instr.* **69** (2020), 101350 (2020).
21. K. Hochberg, S. Becker, M. Louis, P. Klein, and J. Kuhn, "Using smartphones as experimental tools—A follow-up: Cognitive effects by video analysis and reduction of cognitive load by multiple representations," *J. Sci. Educ. Technol.* **29** (2), 303–317 (2020).
22. S. Becker, A. Gößling, P. Klein, and J. Kuhn, "Investigating dynamic visualizations of multiple representations using mobile video analysis in physics lessons: Effects on emotion, cognitive load and conceptual understanding," *Zeitschrift für Didaktik der Naturwissenschaften* **26**, 123–142 (2020).

Technische Universität Technische Universität Kaiserslautern, and Institut für Schule, Erziehungs- und Fachwissenschaften, Bielefeld, Germany; alexander.goessling@gmx.de